

Characterization of Unruh Channel in the context of Open Quantum Systems

Subhashish Banerjee* and Ashutosh Kumar Alok†
Indian Institute of Technology Jodhpur, Jodhpur 342011, India

S. Omkar‡
Indian Institute of Science Education and Research, Thiruvananthapuram, India

R. Srikanth§
Poornaprajna Institute of Scientific Research, Sadashivnagar, Bengaluru- 560080, India

We show through the Choi matrix approach that the effect of Unruh acceleration on a qubit is similar to the interaction of the qubit with a vacuum bath, despite the finiteness of the Unruh temperature. Thus, rather counterintuitively, from the perspective of decoherence in this framework, the particle experiences a vacuum bath with a temperature-modified interaction strength, rather than a thermal bath. We investigate how this “relativistic decoherence” is modified by the presence of environmentally induced decoherence, by studying the degradation of quantum information, as quantified by parameters such as nonlocality, teleportation fidelity, entanglement, coherence and quantum measurement-induced disturbance (a discord-like measure). Also studied are the performance parameters such as gate and channel fidelity. We highlight the distinction between dephasing and dissipative environmental interactions, by considering the actions of quantum non-demolition and squeezed generalized amplitude damping channels, respectively, where, in particular, squeezing is shown to be a useful quantum resource.

I. INTRODUCTION

Quantum information is emerging in the forefront of processing and harnessing of information, using the advantages of quantum mechanics, as well as becoming an essential ingredient towards understanding the fundamental aspects of nature. Relativistic quantum information is a natural quest in this direction [1–7]. In this context, Unruh effect [8, 9] which predicts thermal effects from observing uniform acceleration of the Minkowski vacuum has attracted intense interest [10–14].

Experimental progress in this direction is now attracting considerable attention from the community. Circuit quantum electrodynamics (cQED), using Superconducting Quantum Interferometric Devices (SQUIDS), is a promising effort in this direction. Here tuneable boundary conditions are possible, corresponding to mirrors moving at speeds close to the speed of light in the medium. This was used to experimentally simulate the scenario of dynamical Casimir effect [15], hitherto belonging to the regime of quantum field theory. This paved the way for investigations into various facets of relativistic quantum information. Thus, for example, there have been investigations into relativistic quantum teleportation [16], entanglement generation and gate operations using superconducting resonators [17, 18], entanglement generation via the dynamical Casimir effect using SQUID [19, 20], relativistic effects with superconducting qubits [21] and universal quantum computation, using continuous variable Gaussian cluster states, through relativistic motion of cavity mirrors [22]. Further, there have been investigations of twin paradox in superconducting circuits [23] as well as using the geometric phase to detect the Unruh temperature at accelerations small enough to be experimentally feasible [24]. There have also been investigations into the quantum metrology aspects of Unruh effect [25–27].

This sets the scene for the present investigation where the effect of environmentally induced decoherence, an inevitable attribute for an experimental realization, on various facets of quantum information, as quantified by parameters such as nonlocality, teleportation fidelity, entanglement, coherence and quantum measurement-induced disturbance (a discord-like measure) are studied. We highlight the distinction between dephasing and dissipative environmental interactions, by considering the actions of quantum non-demolition (QND) and squeezed generalized amplitude damping (SGAD) channels, respectively. The QND channel is a purely quantum effect incorporating de-

*Electronic address: subhashish@iitj.ac.in

†Electronic address: akalok@iitj.ac.in

‡Electronic address: omkar.shrm@gmail.com

§Electronic address: srik@poornaprajna.org

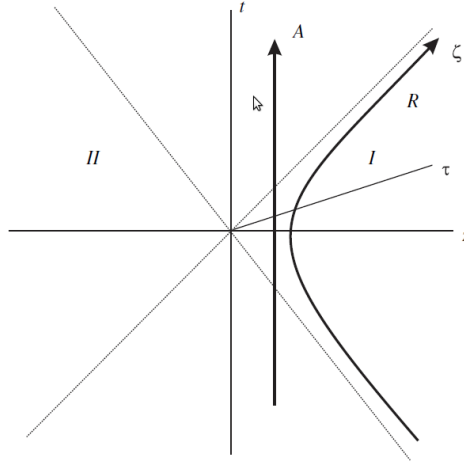


FIG. 1: Minkowski space

coherence without dissipation [28], tracing its roots to gravitational wave detection [29, 30]. The SGAD [31, 32] is a very general dissipative channel of the Lindblad class and incorporates the well known amplitude damping (AD) and generalized amplitude damping (GAD) channels as limiting cases. In [33], the pure Unruh channel for the Dirac qubit, that is, the Unruh channel without any external influence, was characterized information theoretically by constructing its Kraus operators. Here, the Unruh channel is quantified taking into account possible ambient external influences. Useful parameters characterizing channel performance are the gate fidelity [34] as well as the average gate fidelity [32, 35, 36]. They represent how well a (noisy) gate performs the operation it is supposed to implement. How well a gate preserves the distinguishability of states is captured by another channel performance parameter, the channel fidelity, introduced in [31]. These channel parameters are applied here to the Unruh channel, both with and without external influences.

The plan of the work is as follows. In Section II, we briefly discuss the Unruh channel for the Dirac qubit with emphasis towards its information theoretic characterization. This is followed by studying how external influences, characterized by parameters like temperature, squeezing and evolution time, effect various features of quantum information, such as nonlocality, entanglement, teleportation fidelity and measurement-induced disturbance. Next, the average gate and channel fidelities are studied in order to gain insight into the nature of the Unruh channel. Quantum coherence, characteristic of a quantum operation, as a resource theory has attracted a lot of attention in recent times. Mixing, which is inevitable with evolution, will result in a degradation of coherence. In order to have an operational estimation of the utility of a quantum task, it is imperative to have an understanding of the trade-off between the two [38–40]. This is done for the Unruh channel, pure as well as in the presence of ambient effects, in the penultimate section. We then make our conclusions.

II. INVITATION TO UNRUH EFFECT

We consider two observers, Alice (A) and Rob (R) sharing a maximally entangled initial state of two qubits at a point in flat Minkowski spacetime. Then Rob moves with a uniform acceleration and Alice stays stationary. Moreover, we assume that the observers are equipped with detectors that are sensitive only to their respective modes and share the following maximally entangled initial state:

$$|\psi\rangle_{A,R} = \frac{|00\rangle_{A,R} + |11\rangle_{A,R}}{\sqrt{2}}. \quad (1)$$

Assuming that R gets uniformly accelerated with acceleration a , from R's frame the Minkowski vacuum state is a two mode squeezed state [11]:

$$|0\rangle_M = \cos(r)|0\rangle_I|0\rangle_{II} + \sin(r)|1\rangle_I|1\rangle_{II}, \quad (2)$$

and the excited state is

$$|1\rangle_M = \cos(r)|1\rangle_I|1\rangle_{II}, \quad (3)$$

where $\cos(r) = \frac{1}{\sqrt{e^{-\frac{2\pi\omega c}{a}} + 1}}$ and ω is Dirac particle acceleration with c being the speed of light in vacuum.

From the Fig. (1), it can be seen that the regions I and II are causally disconnected. The state in Eq. (1) has contribution from the regions I and II. Since these regions are disconnected, the mode corresponding to II can be traced out to obtain the following density matrix

$$\rho_{A,I} = \frac{1}{2} [\cos^2(r)|00\rangle\langle 00| + \cos(r)(|00\rangle\langle 11| + |11\rangle\langle 00|) + \sin^2(r)|01\rangle\langle 01| + |11\rangle\langle 11|]. \quad (4)$$

Consider the maximally entangled two mode state in which the second mode is Unruh accelerated. The state is represented by

$$\rho_u = \frac{1}{2} \begin{pmatrix} \cos^2 r & 0 & 0 & \cos r \\ 0 & \sin^2 r & 0 & 0 \\ 0 & 0 & 0 & 0 \\ \cos r & 0 & 0 & 1 \end{pmatrix}, \quad (5)$$

where $\sin(r) = \frac{1}{1+e^{\frac{2\pi\omega c}{a}}}$.

Leaving out the factor $1/2$ in ρ_u , the corresponding Choi matrix [43, 44] is $|i\rangle\langle i|\mathcal{E}(|j\rangle\langle j|)$, from which the Kraus representation of the Unruh channel can be obtained. Following the procedure for constructing Kraus operators we have

$$K_1^u = \begin{pmatrix} \cos r & 0 \\ 0 & 1 \end{pmatrix}, \quad K_2^u = \begin{pmatrix} 0 & 0 \\ \sin r & 0 \end{pmatrix}. \quad (6)$$

The above Kraus operators are similar to

$$K_1 = \begin{pmatrix} \sqrt{1-\gamma} & 0 \\ 0 & 1 \end{pmatrix}, \quad K_2 = \begin{pmatrix} 0 & 0 \\ \sqrt{\gamma} & 0 \end{pmatrix}, \quad (7)$$

which represents the dissipative interaction of a qubit with the vacuum bath, i.e., an amplitude damping channel [31, 32]. Here $\gamma = \frac{1}{e^{\frac{\hbar\omega}{k_B T}}}$. Thus, rather surprisingly, from the viewpoint of decoherence, the qubit experiences a vacuum bath, with the role of Unruh temperature being to modify the interaction strength, rather than to serve as bath temperature.

To see what acceleration a simulates the temperature T , let us equate

$$\frac{1}{1 + e^{\frac{2\pi\omega c}{a}}} = \frac{1}{e^{\frac{\hbar\omega}{k_B T}}}. \quad (8)$$

Thus we have the relation between T and a as

$$\frac{\hbar\omega}{k_B T} = \log \left(1 + e^{\frac{2\pi\hbar\omega c}{a}} \right). \quad (9)$$

For small a , 1 in the above equation can be ignored and we have the relation

$$a = 2\pi k_B c T. \quad (10)$$

For $a \rightarrow \infty$, $1 + e^{\frac{2\pi\hbar\omega c}{a}} \rightarrow 2$ and the corresponding temperature is

$$T_\infty = \frac{\hbar\omega}{k_B \log 2}. \quad (11)$$

T_∞ is the maximum temperature that can be simulated by Unruh effect. Since the maximum temperature is never infinite, the asymptotic state due to Unruh acceleration is never a maximally mixed state and entanglement is seen to survive [33]. In contrast, the qubit interacting with a thermal bath can become maximally mixed for infinite bath temperatures.

Once we have the Kraus operators of the Unruh channel, we can calculate its effect on a qubit in pure state given by

$$\rho = \begin{pmatrix} \cos^2(\theta/2) & e^{i\phi} \cos(\theta/2) \sin(\theta/2) \\ e^{-i\phi} \cos(\theta/2) \sin(\theta/2) & \sin^2(\theta/2) \end{pmatrix}. \quad (12)$$

The action of the Unruh channel on the state ρ is

$$\mathcal{E}_u(\rho) = \begin{pmatrix} \cos^2 r \cos^2(\theta/2) & \cos r e^{i\phi} \cos(\theta/2) \sin(\theta/2) \\ \cos r e^{-i\phi} \cos(\theta/2) \sin(\theta/2) & \sin^2 r \cos^2(\theta/2) + \sin^2(\theta/2) \end{pmatrix}. \quad (13)$$

III. DEGRADATION OF QUANTUM INFORMATION UNDER UNRUH CHANNEL

The nonclassicality of quantum information can be characterized in terms of nonlocality B (for e.g., Bell inequality violation [45–50]), entanglement, characterized here by concurrence C [51], teleportation fidelity F_{max} [49, 52, 53] or weaker nonclassicality measures like quantum discord D [54] or measurement induced disturbance M [55]. In the accelerated reference frame, the Unruh effect degrades the quantumness of the state (4) [27, 33]. To achieve our goal, we consider the scenario wherein only Robs qubit is interacting with a noisy environment. The other case in which both the qubits of the two observers interact with a noisy environment is not seen here to produce any qualitatively useful insight and hence is not considered in what follows.

A. Effect of QND noise

QND is a purely dephasing noise channel whose action on a qubit, characterized by frequency ω_0 , can be studied using the following Kraus operators [28]

$$K_1 = \sqrt{\frac{1 - e^{-\omega_0 \gamma^2(t)}}{2}} \begin{pmatrix} e^{i\omega_0 t} & 0 \\ 0 & -1 \end{pmatrix}; \quad K_2 = \sqrt{\frac{1 + e^{-\omega_0 \gamma^2(t)}}{2}} \begin{pmatrix} e^{i\omega_0 t} & 0 \\ 0 & 1 \end{pmatrix}. \quad (14)$$

Assuming an Ohmic bath spectral density with an upper cut-off frequency ω_c , it can be shown that

$$\begin{aligned} \gamma(t) = & \left(\frac{\gamma_0 k_B T}{\pi \hbar \omega_c} \right) \cosh(2s) \left(2\omega_c t \tan^{-1}(\omega_c t) + \ln \left[\frac{1}{1 + \omega_c^2 t^2} \right] \right) \\ & - \left(\frac{\gamma_0 k_B T}{2\pi \hbar \omega_c} \right) \sinh(2s) \left(4\omega_c(t-a) \tan^{-1}[2\omega_c(t-a)] - 4\omega_c(t-2a) \tan^{-1}[\omega_c(t-2a)] \right. \\ & \left. + 4a\omega_c \tan^{-1}(2a\omega_c) + \ln \left[\frac{(1 + \omega_c^2(t-2a)^2)^2}{1 + 4\omega_c^2(t-a)^2} \right] + \ln \left[\frac{1}{1 + 4a^2\omega_c^2} \right] \right). \end{aligned} \quad (15)$$

Here T is the reservoir temperature, while a and s are bath squeezing parameters. Now, the corresponding Choi matrix have the form

$$\begin{pmatrix} \cos^2 r & 0 & 0 & e^{i\omega_0 t} e^{-\omega_0 \gamma^2(t)} \cos r \\ 0 & \sin^2 r & 0 & 0 \\ 0 & 0 & 0 & 0 \\ e^{-i\omega_0 t} e^{-\omega_0 \gamma^2(t)} \cos r & 0 & 0 & 1 \end{pmatrix}, \quad (16)$$

The new Kraus operators are

$$\begin{aligned} K_1 &= \frac{\sqrt{\cos 2r + 3 - 2e^{-\frac{1}{4}(\gamma\omega^2)}\sqrt{\mathcal{A}}}}{2\sqrt{\frac{1}{4}\sec^2 r \left(\sqrt{\mathcal{A}} + e^{\frac{\gamma\omega^2}{4}} \sin^2 r \right)^2 + 1}} \times \begin{pmatrix} -\frac{1}{2}e^{it\omega} \sec r \left(\sqrt{\mathcal{A}} + e^{\frac{1}{4}\omega^2\gamma} \sin^2 r \right) & 0 \\ 0 & 1 \end{pmatrix} \\ K_2 &= \frac{\sqrt{\cos 2r + 3 + 2e^{-\frac{1}{4}(\gamma\omega^2)}\sqrt{\mathcal{A}}}}{2\sqrt{\frac{1}{4}\sec^2 r \left(\sqrt{\mathcal{A}} - e^{\frac{\gamma\omega^2}{4}} \sin^2(r) \right)^2 + 1}} \times \begin{pmatrix} \frac{1}{2}e^{it\omega} \sec r \left(\sqrt{\mathcal{A}} - e^{\frac{1}{4}\omega^2\gamma} \sin^2 r \right) & 0 \\ 0 & 1 \end{pmatrix} \\ K_3 &= \begin{pmatrix} 0 & 0 \\ \sin r & 0 \end{pmatrix}, \end{aligned} \quad (17)$$

where $\mathcal{A} = e^{\frac{\gamma\omega^2}{2}} \sin^4 r + 2\cos 2r + 2$ and the Kraus operators satisfy the completeness $\sum_i^3 K_i^\dagger K_i = \mathbb{I}$.

For the initial time $t = 0$, when the QND interaction has not begun, $e^{-\omega_0 \gamma^2(t)} = 1$ and the above Kraus operators reduce to that in Eq. (6). The composition of the dephasing channel with the Unruh channel has 3 Kraus operators, essentially because only three of the resulting four operators obtained under composition, are linearly independent. To see this, let the two Kraus operators of the amplitude damping channel be denoted

$$\mathcal{A}_1 \equiv \begin{pmatrix} 1 & 0 \\ 0 & \sqrt{1-\lambda} \end{pmatrix}, \quad \mathcal{A}_2 \equiv \begin{pmatrix} 0 & 0 \\ \sqrt{\lambda} & 0 \end{pmatrix},$$

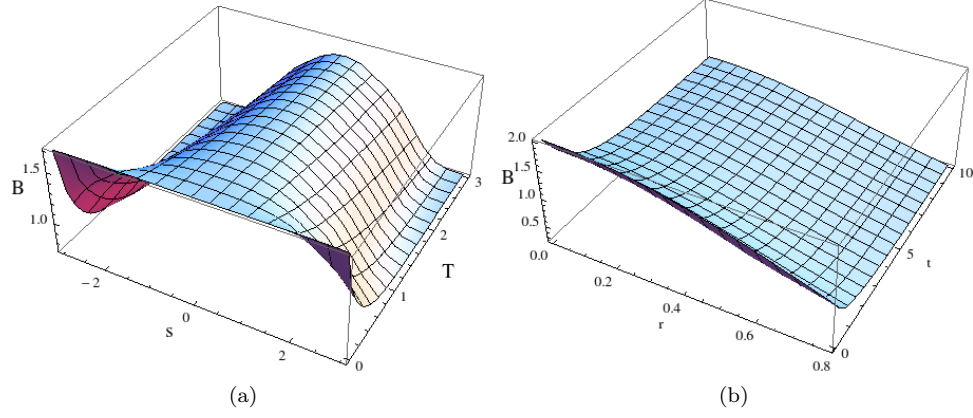


FIG. 2: (a) Plot of Bell's inequality B against temperature T and squeezing s when Robs accelerated qubit interacts dissipatively with the environment. Robs acceleration corresponds to $r = \pi/8$ and $t = 0.5$. (b) Plot of Bell's inequality B against time t for which QND channel acts and r . The bath parameters are $\omega_0 = 1$, the coupling $\gamma = 0.1$ and squeezing angle $\phi = 0$, $T = 0.5$ and $s = 0.5$.

and those for the dephasing channel by

$$\mathcal{D}_1 \equiv \sqrt{p} \begin{pmatrix} 1 & 0 \\ 0 & 1 \end{pmatrix}, \quad \mathcal{D}_2 \equiv \sqrt{1-p} \begin{pmatrix} 1 & 0 \\ 0 & -1 \end{pmatrix}.$$

The composition of these two channels has the Kraus operators $\mathcal{D}_1\mathcal{A}_1$, $\mathcal{D}_2\mathcal{A}_1$, $\mathcal{D}_1\mathcal{A}_2$ and $\mathcal{D}_2\mathcal{A}_2$, where the last two terms, namely,

$$\mathcal{D}_1\mathcal{A}_2 = \sqrt{p\lambda} \begin{pmatrix} 0 & 0 \\ 1 & 0 \end{pmatrix} \quad \text{and} \quad \mathcal{D}_2\mathcal{A}_2 = \sqrt{p\lambda} \begin{pmatrix} 0 & 0 \\ -1 & 0 \end{pmatrix}, \quad (18)$$

are equivalent in that they produce the same noise effect. Thus, the composed noise channel has a rank of three corresponding to the indepenent Kraus operators $\mathcal{D}_1\mathcal{A}_1$, $\mathcal{D}_2\mathcal{A}_1$, and $\mathcal{D}_1\mathcal{A}_2$ or $\mathcal{D}_2\mathcal{A}_2$.

The QND channel acting on the Unruh qubit effects its quantum characteristics and can be studied by the behavior of the different facets of quantum correlations. For the case of QND noise acting on Rob, analytical expressions can be obtained for the corresponding measures of quantum correlations which are as follows,

$$\begin{aligned} M = & \frac{1}{8} \left[4 + \frac{3 + \cos 2r - 2\sqrt{4e^{-\omega_0^2\gamma^4(t)} \cos^2 r + \sin^4 r}}{8} \log \left(\frac{3 + \cos 2r - 2\sqrt{4e^{-\omega_0^2\gamma^4(t)} \cos^2 r + \sin^4 r}}{8} \right) \right. \\ & + \frac{3 + \cos 2r + 2\sqrt{4e^{-\omega_0^2\gamma^4(t)} \cos^2 r + \sin^4 r}}{8} \log \left(\frac{3 + \cos 2r + 2\sqrt{4e^{-\omega_0^2\gamma^4(t)} \cos^2 r + \sin^4 r}}{8} \right) \\ & \left. - 4 \cos^2 r \log \left(\frac{\cos^2 r}{2} \right) \right], \end{aligned} \quad (19)$$

$$F_{\max} = \frac{1}{2} \left[1 + \frac{\cos r}{3} \left(2e^{-\omega_0\gamma^2(t)} + \cos r \right) \right], \quad (20)$$

$$B = 2e^{-\omega_0^2\gamma^4(t)} \cos^2 r. \quad (21)$$

The analytical expression for entanglement C turns out to be very involved. Hence we only provide a numerical analysis. For the initial time $t = 0$ when QND interaction has not begun, $e^{-\omega_0\gamma^2(t)} = 1$ and the expressions F_{\max} , B and M in the above equations reduce to the pure Unruh-effect case.

The figures 2 to 5 correspond to the behavior of various aspects of quantum correlations of the Unruh channel under the influence of QND noise. It can be seen from Fig. 2(a) that as reservoir squeezing s increases, the channel becomes

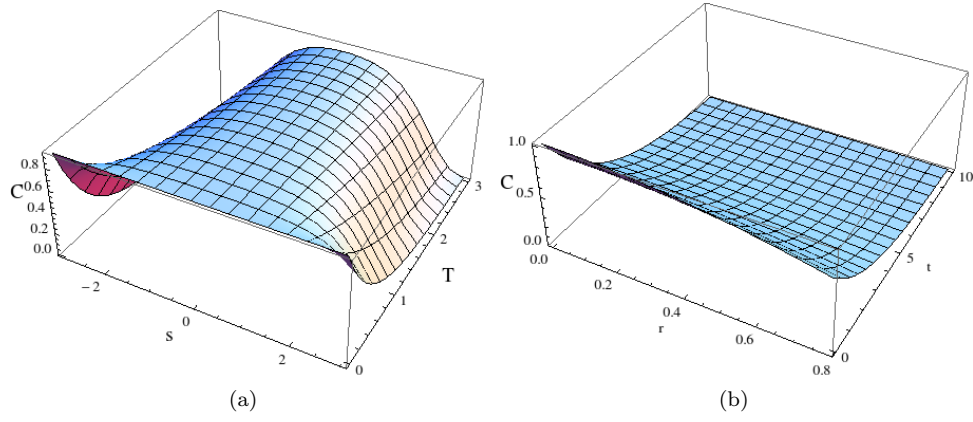


FIG. 3: (a) Plot of concurrence C against temperature T and squeezing s when Robs accelerated qubit is subjected to a QND channel. Robs acceleration corresponds to $r = \pi/8$ and $t = 0.5$. (b) Plot of C against time t for which QND channel acts and r . The bath parameters are $\omega_0 = 0.1$, the coupling $\gamma = 0.1$ and squeezing angle $\phi = 0$, $T = 1.5$ and $s = 1.5$.

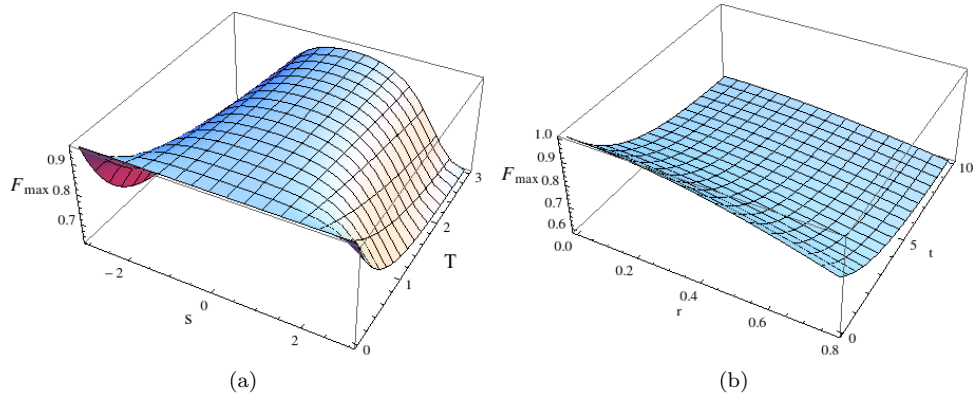


FIG. 4: (a) Plot of teleportation fidelity F_{\max} against temperature T and squeezing s when Robs accelerated qubit is subjected to a QND channel. Robs acceleration corresponds to $r = \pi/8$, $t = 0.5$. (b) Plot of F_{\max} against time t for which QND channel acts and r . The bath parameters are $\omega_0 = 1$, the coupling $\gamma = 0.1$ and squeezing angle $\phi = 0$, $T = 1.5$ and $s = 1.5$.

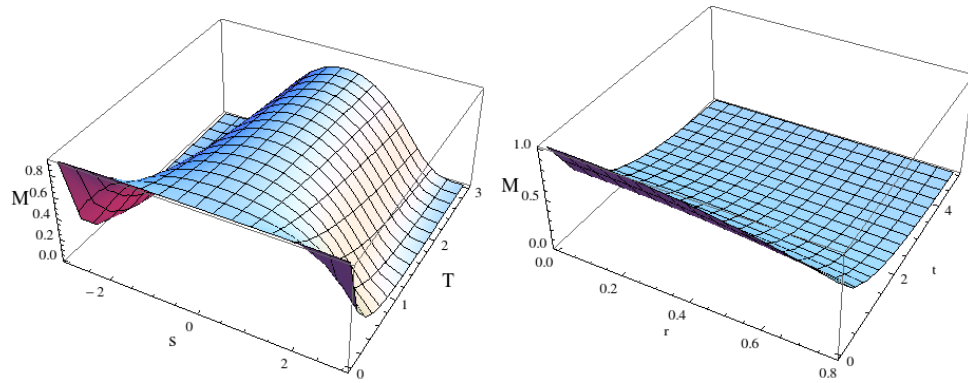


FIG. 5: (a) Plot of M against temperature T and squeezing s when Robs accelerated qubit is subjected to a QND channel. Robs acceleration corresponds to $r = \pi/8$ and $t = 0.5$. (b) Plot of M against time t for which QND channel acts and r . The bath parameters are $\omega_0 = 1$, the coupling $\gamma = 0.1$ and squeezing angle $\phi = 0$, $T = 1.5$ and $s = 1.5$.

local even for a small external temperature T . Also, from Fig. 2(b) the channel is seen to become local with increase in the Unruh acceleration depicted, here, by r . Entanglement is seen, in Fig. 3(a), to decrease with increase in s . This feature is more prominent for $T > 1$. From Fig. 3(b), for a given value of r , entanglement is seen to decrease with time. For $|s| < 2$, Fig. 4(a) shows that $F_{\max} > \frac{2}{3}$ for the given temperature range. Also, F_{\max} decreases with increase in r and time of evolution t , Fig. 4(b). M , Fig. 5, is seen to decrease with increase in the parameters t , s , T and r .

B. Effect of SGAD noise

The Kraus corresponding to the SGAD channel are

$$\begin{aligned} K_1 &\equiv \sqrt{p_1} \begin{bmatrix} \sqrt{1-\alpha} & 0 \\ 0 & 1 \end{bmatrix}, & K_2 &\equiv \sqrt{p_1} \begin{bmatrix} 0 & 0 \\ \sqrt{\alpha} & 0 \end{bmatrix}, \\ K_3 &\equiv \sqrt{p_2} \begin{bmatrix} \sqrt{1-\mu} & 0 \\ 0 & \sqrt{1-\nu} \end{bmatrix}, & K_4 &\equiv \sqrt{p_2} \begin{bmatrix} 0 & \sqrt{\nu} \\ \sqrt{\mu}e^{-i\phi_s} & 0 \end{bmatrix}, \end{aligned} \quad (22)$$

where $p_1 + p_2 = 1$ [31]. Here

$$\begin{aligned} p_2 &= \frac{1}{(A+B-C-1)^2 - 4D} \times [A^2B + C^2 + A(B^2 - C - B(1+C) - D) - (1+B)D \\ &\quad - C(B+D-1) \pm 2\sqrt{D(B-AB+(A-1)C+D)(A-AB+(B-1)C+D)}], \end{aligned} \quad (23)$$

where

$$\begin{aligned} A &= \frac{2N+1}{2N} \frac{\sinh^2(\gamma_0 at/2)}{\sinh(\gamma_0(2N+1)t/2)} \exp(-\gamma_0(2N+1)t/2), \quad B = \frac{N}{2N+1} (1 - \exp(-\gamma_0(2N+1)t)), \\ C &= A + B + \exp(-\gamma_0(2N+1)t), \quad D = \cosh^2(\gamma_0 at/2) \exp(-\gamma_0(2N+1)t). \end{aligned} \quad (24)$$

Also,

$$\begin{aligned} \nu &= \frac{N}{(p_2)(2N+1)} (1 - e^{-\gamma_0(2N+1)t}), \quad \mu = \frac{2N+1}{2(p_2)N} \frac{\sinh^2(\gamma_0 at/2)}{\sinh(\gamma_0(2N+1)t/2)} \exp\left(-\frac{\gamma_0}{2}(2N+1)t\right), \\ \alpha &= \frac{1}{p_1} \left(1 - p_2[\mu(t) + \nu(t)] - e^{-\gamma_0(2N+1)t}\right). \end{aligned} \quad (25)$$

Also $N = N_{\text{th}}[\cosh^2(s) + \sinh^2(s)] + \sinh^2(s)$, $a = \sinh(2s)(2N_{\text{th}} + 1)$ where $N_{\text{th}} = 1/(e^{\hbar\omega_0/k_B T} - 1)$ is the Planck distribution giving the number of thermal photons at the frequency ω_0 ; s and ϕ_s are bath squeezing parameters.

The analytical expressions are complicated and hence we resort to numerical discussions. The figures 6 - 9 correspond to the behavior of various aspects of quantum correlations of the Unruh channel under the influence of SGAD noise. From Fig. 6(a) it can be seen that for certain range of T , squeezing enhances B . However, for the values of the parameters indicated, it never crosses the threshold of nonlocality ($B > 1$). From Fig. 6(b) it can be seen that with increase in r and t , B decreases and the channel becomes local. From Fig. 7(a), concurrence is seen to drop drastically to zero with increase in T . Also for large values of s , concurrence is seen to fall to zero, irrespective of T . Fig. 7(b) depicts the decrease of concurrence with respect to time for any give value of r . From Fig. 8, F_{\max} is seen to decrease with T , s , r and t . From Fig. 9, M is seen to decrease with increase in the parameters r and t . However for certain range of T , M is seen to increase with bath squeezing s , reiterating the usefulness of squeezing.

IV. AVERAGE GATE AND CHANNEL FIDELITY

In this work we are trying to understand the Unruh channel under the influence of external noisy effects. From the perspective of quantum information, a useful way to understand this is to analyze the average gate and channel fidelities [32] of the Unruh channel under the ambient environmental conditions.

The average gate fidelity [31, 57–59] has a closed expression

$$G_{\text{av}} = \frac{d + \sum_i |\text{Tr}(E_i)|^2}{d(d+1)}. \quad (26)$$

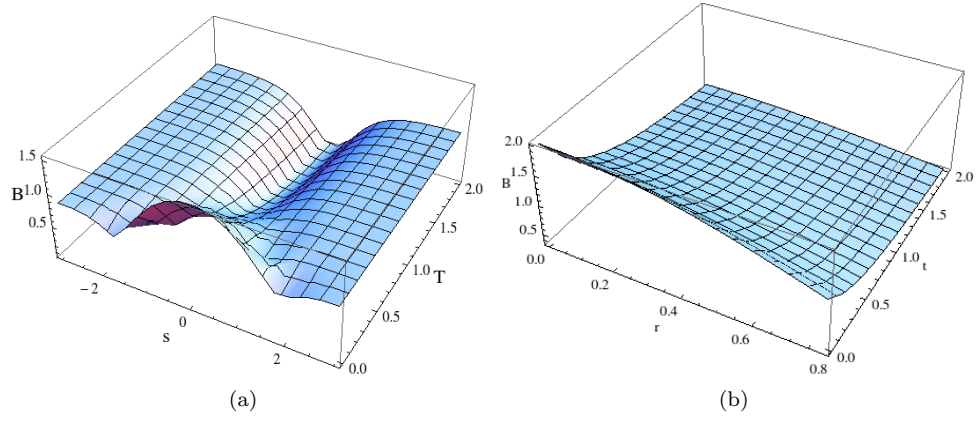


FIG. 6: (a) Plot of Bell's inequality B against temperature T and squeezing s when Robs accelerated qubit is subjected to a SGAD channel. Robs acceleration corresponds to $r = \pi/8$. (b) Plot of Bell's inequality B against time t for which SGAD channel acts and r . The bath parameters are $\omega_0 = 0.1$, the coupling $\gamma = 0.1$ and squeezing angle $\phi = 0$, $T = 0.5$ and $s = 0.5$.

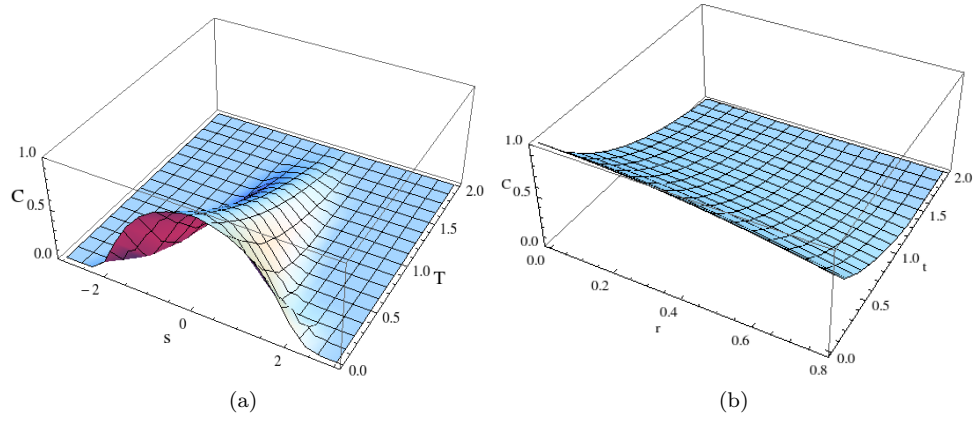


FIG. 7: (a) Plot of concurrence C against temperature T and squeezing s when Robs accelerated qubit is subjected to a SGAD channel. Robs acceleration corresponds to $r = \pi/8$. (b) Plot of C against time t for which SGAD channel acts and r . The bath parameters are $\omega_0 = 0.1$, the coupling $\gamma = 0.1$ and squeezing angle $\phi = 0$, $T = 0.5$ and $s = 0.5$.

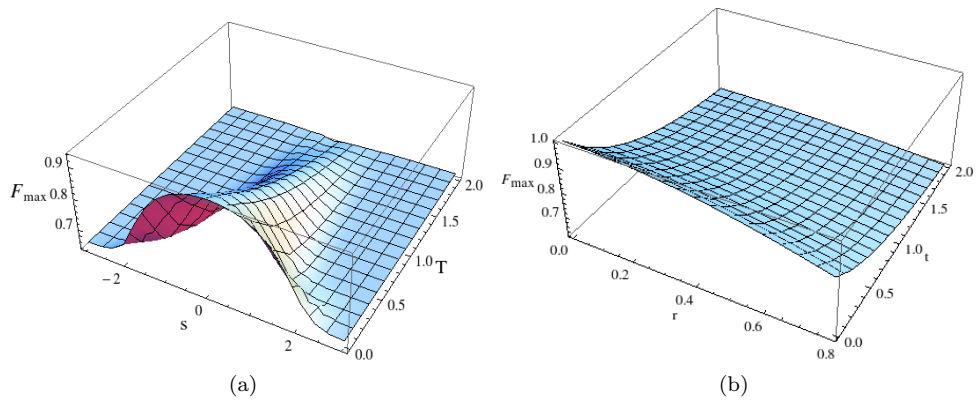


FIG. 8: (a) Plot of teleportation fidelity F_{\max} against temperature T and squeezing s when the Robs accelerated qubit is subjected to a SGAD channel. Robs acceleration corresponds to $r = \pi/8$. (b) Plot of F_{\max} against time t for which SGAD channel acts and r . The bath parameters are $\omega_0 = 0.1$, the coupling $\gamma = 0.1$ and squeezing angle $\phi = 0$, $T = 0.5$ and $s = 0.5$.

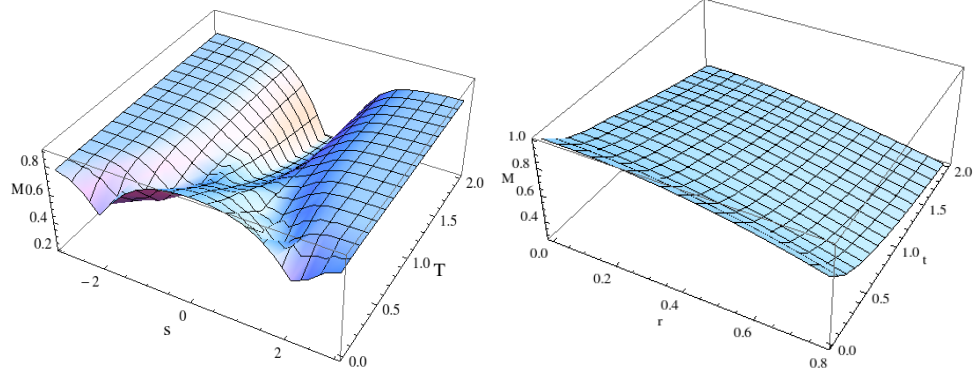


FIG. 9: (a) Plot of MID M against temperature T and squeezing s when the Robs accelerated qubit is subjected to a SGAD channel. Robs acceleration corresponds to $r = \pi/8$ and $t = 0.5$. (b) Plot of M against time t for which SGAD channel acts and r . The bath parameters are $\omega_0 = 0.1$, the coupling $\gamma = 0.1$ and squeezing angle $\phi = 0$, $T = 0.5$ and $s = 0.5$.

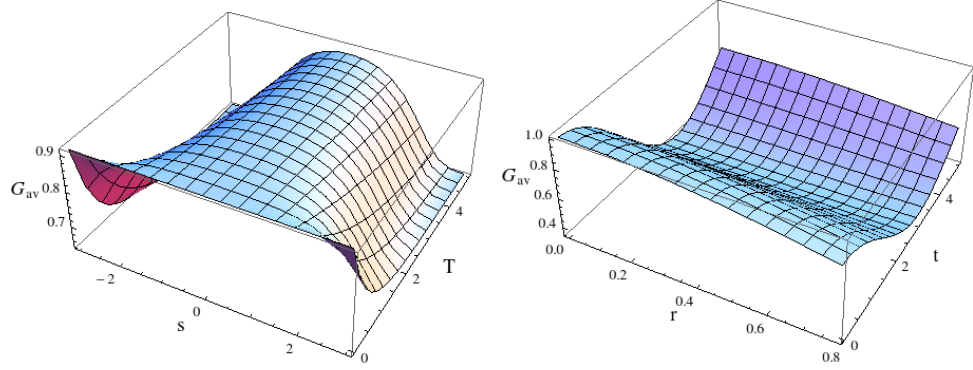


FIG. 10: (a) Plot of average gate fidelity G_{av} against temperature T and squeezing s when Robs accelerated qubit is subjected to a QND channel. Robs acceleration corresponds to $r = \pi/8$ and $t = 0.5$. (b) Plot of G_{av} against time t for which QND channel acts and r . The bath parameters are $\omega_0 = 1$, the coupling $\gamma = 0.1$ and squeezing angle $\phi = 0$, $T = 0.5$ and $s = 0.5$.

For the Unruh channel $G_{av} = \frac{1}{6} (2 + (1 + \cos r)^2)$, where d is the dimensionality of the system on which channel \mathcal{E} acts with operator sum representation elements E_i .

For the QND-Unruh channel

$$\begin{aligned}
 |\text{Tr}(E_i)|^2 = & \frac{\left(2\sqrt{\mathcal{A}}e^{-\frac{1}{4}\gamma\omega_0^2} + \cos 2r + 3\right) \left(\sec r \cos \omega_0 t \left(\sqrt{\mathcal{A}} - e^{\frac{\gamma\omega_0^2}{4}} \sin^2 r\right) + \frac{1}{4} \sec^2 r \left(\sqrt{\mathcal{A}} - e^{\frac{\gamma\omega_0^2}{4}} \sin^2 r\right)^2 + 1\right)}{\sec^2 r \left(\sqrt{\mathcal{A}} - e^{\frac{\gamma\omega_0^2}{4}} \sin^2 r\right)^2 + 4} \\
 & + \frac{\left(-2\sqrt{\mathcal{A}}e^{-\frac{1}{4}\gamma\omega_0^2} + \cos r + 3\right) \left(-\sec r \cos \omega_0 t \left(\sqrt{\mathcal{A}} + e^{\frac{\gamma\omega_0^2}{4}} \sin^2 r\right) + \frac{1}{4} \sec^2 r \left(\sqrt{\mathcal{A}} + e^{\frac{\gamma\omega_0^2}{4}} \sin^2 r\right)^2 + 1\right)}{\sec^2 r \left(\sqrt{\mathcal{A}} + e^{\frac{\gamma\omega_0^2}{4}} \sin^2 r\right)^2 + 4}, \quad (27)
 \end{aligned}$$

using which G_{av} can be calculated. In the limit $t \rightarrow 0$ this reduces to the Unruh case. Unlike the QND case, the analytical expression for G_{av} for the SGAD channel is very involved, and hence we discuss this case numerically.

From Fig. 10(a), it can be seen that G_{av} is stable for a certain range of squeezing, after which it falls. G_{av} is also seen to decrease with r . However with time, G_{av} first decreases and then is then seen to increase. Since the expression for G_{av} has the oscillatory term $\cos \omega_0 t$, oscillation is seen in Fig. 10(b) with time t .

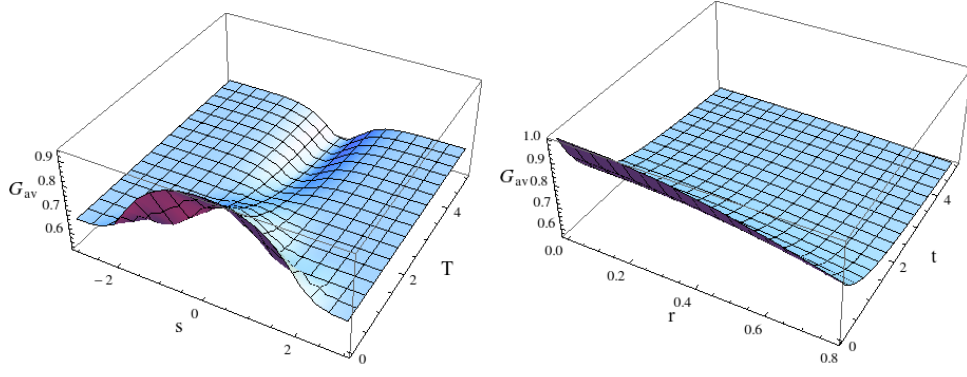


FIG. 11: (a) Plot of average gate fidelity G_{av} against temperature T and squeezing s when Robs accelerated qubit is subjected to a SGAD channel. Robs acceleration corresponds to $r = \pi/8$ and $t = 0.5$. (b) Plot of G_{av} against time t for which SGAD channel acts and r . The bath parameters are $\omega_0 = 0.1$, the coupling $\gamma = 0.1$ and squeezing angle $\phi = 0$, $T = 0.5$ and $s = 0.5$.

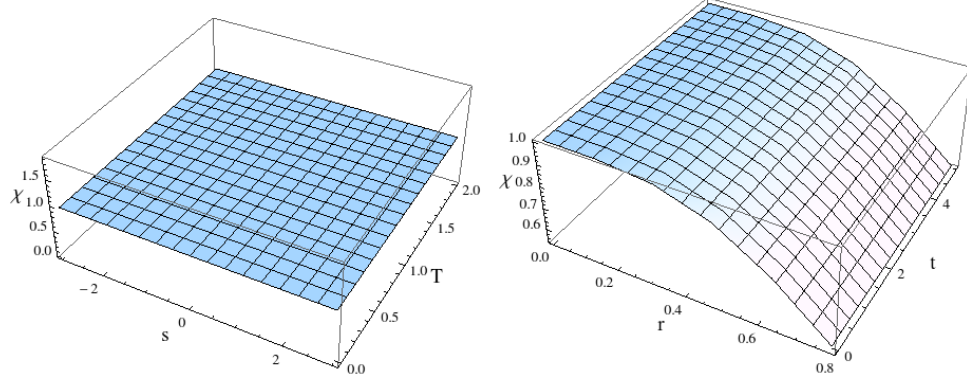


FIG. 12: (a) Plot of channel fidelity χ against temperature T and squeezing s when Robs accelerated qubit is subjected to a QND channel. Robs acceleration corresponds to $r = \pi/8$ and $t = 0.5$. (b) Plot of χ against time t for which QND channel acts and r . The bath parameters are $\omega_0 = 1$, the coupling $\gamma = 0.1$ and squeezing angle $\phi = 0$, $T = 0.5$ and $s = 0.5$.

From Figs. 11, a general trend is observed of average gate fidelity G_{av} , under the influence of the SGAD channel, decreasing with increase in T as well as evolution time t , for a given r . However, as can be observed from Fig. 11(a), for a certain range of T , G_{av} is seen to increase with reservoir squeezing s . This indicates that squeezing can be a useful quantum resource in this scenario.

Another quantity frequently used to access the channel's performance is the channel fidelity [31, 32]

$$\chi = \max_{\mathcal{B}} \kappa(\mathcal{B}, \mathcal{E}), \quad (28)$$

where $\kappa(\mathcal{B}, \mathcal{E})$ is the Holevo bound for states prepared in basis \mathcal{B} and passed through the channel \mathcal{E} . The maximum is achieved for the states prepared in the basis $\{|0\rangle, |1\rangle\}$, i.e., for the state $\frac{1}{2}(|0\rangle\langle 0| + |1\rangle\langle 1|)$. κ signifies how well the quantum input states are distinguishable after the action of the channel \mathcal{E} . It can also be interpreted as how much classical information can be extracted from the given quantum ensemble.

From Fig. 12 it can be seen that χ , for the Unruh-QND channel, does not change with s , T and t . The reason is that the maximum is obtained for completely mixed state with no off-diagonal terms which make the QND ineffective, whereas the diagonal terms are altered by the Unruh effect. For the Unruh-SGAD channel, we see from Fig. 13(a) that the Unruh channel drives the state away from the maximally mixed state for which the Holevo bound is maximum. By increasing the bath squeezing and the temperature the system is driven back towards the maximally mixed states which results in increment of χ to its maximum value. Fig. 13(b) show that as the SGAD channel acts for longer duration the state is driven towards maximally mixed state and thus χ increases with t .

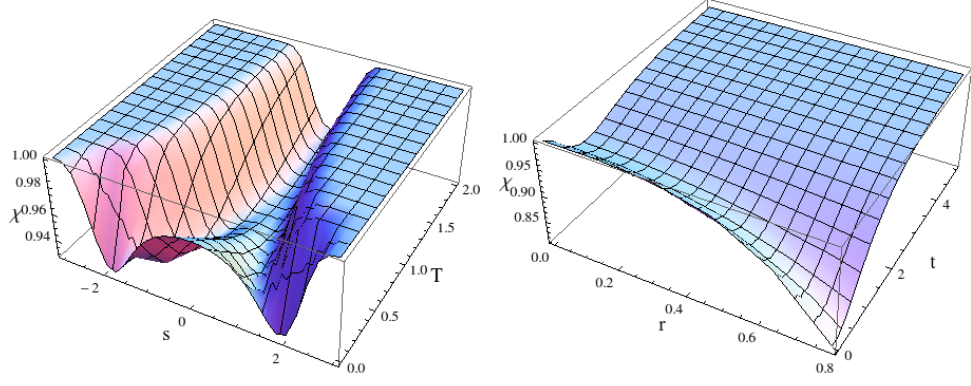


FIG. 13: (a) Plot of channel fidelity χ against temperature T and squeezing s when Robs accelerated qubit is subjected to a SGAD channel. Robs acceleration corresponds to $r = \pi/8$ and $t = 0.5$. (b) Plot of χ against time t for which SGAD channel acts and r . The bath parameters are $\omega_0 = 0.1$, the coupling $\gamma = 0.1$ and squeezing angle $\phi = 0$, $T = 0.5$ and $s = 0.5$.

V. COHERENCE AND MIXEDNESS

Quantum coherence as a resource has attracted much attention in recent times [38–40]. Coherence plays a central role in quantum mechanics [5] enabling operations or tasks which are impossible within the regime of classical mechanics.

For a quantum state represented by density matrix ρ in basis $\{|i\rangle\}$, the l_1 norm of coherence is given by

$$\mathcal{C}(\rho) = \sum_{i \neq j} |\rho_{i,j}|. \quad (29)$$

The mixedness, which is basically normalized linear entropy, of a d dimensional quantum state ρ is given by [56]

$$\mathcal{M}(\rho) = \frac{d}{d-1} (1 - \text{Tr} \rho^2). \quad (30)$$

The inequality relation between the $\mathcal{C}(\rho)$ and $\mathcal{M}(\rho)$ is [40]

$$\frac{\mathcal{C}(\rho)^2}{(d-1)^2} + \mathcal{M}(\rho) \leq 1. \quad (31)$$

When this inequality is saturated for certain values of $\mathcal{C}(\rho)$ and $\mathcal{M}(\rho)$, the situation corresponds to states which have maximum coherence for a given mixedness in the states. Such states are known as Maximally Coherent Mixed States (MCMS).

A. QND Channel

The analytical expressions for coherence and mixedness of the Unruh channel under the influence of the QND noise are

$$\mathcal{C}(\rho) = \cos \frac{\theta}{2} \sin \frac{\theta}{2} \cos^r e^{-\frac{\omega_0^2 \gamma(t)}{4}}, \quad (32)$$

$$\mathcal{M}(\rho) = \cos^2 r \left(\cos^2 \frac{\theta}{2} (3 - \cos 2r - 2 \cos^2 r \cos \theta) - e^{-\frac{\omega_0^2 \gamma(t)}{2}} \sin^2 \theta \right), \quad (33)$$

respectively.

From Fig. 14, coherence \mathcal{C} is seen to decrease with increase in temperature T as well as reservoir squeezing s . Mixing \mathcal{M} increases with both T and s . From Fig. 15, it can be seen that coherence decreases with t whereas mixedness increases with t as well as r , a feature which is consistent with common intuition.

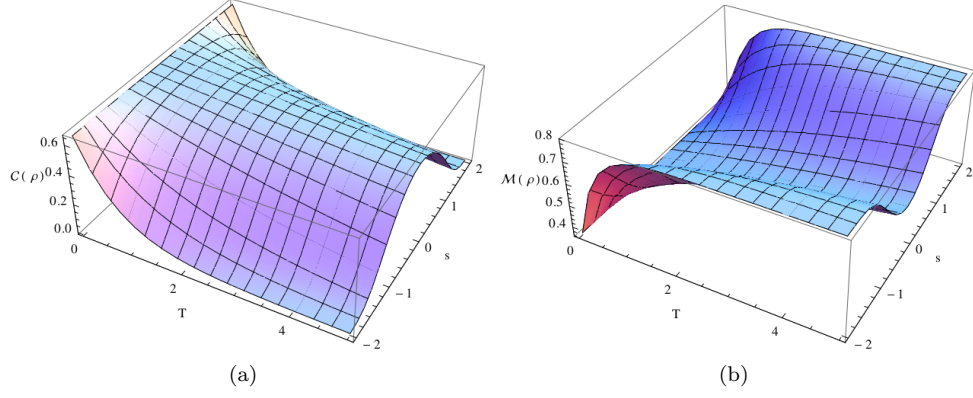


FIG. 14: (a) Variation of Coherence due to action of QND channel with bath squeezing (s) and temperature (T). (b) Variation of Mixedness plotted against s and T . The bath parameters are $a = 0$, $\omega_0 = 1$, $\gamma = 0.1$, $t = 2$, $r = \pi/8$ and the input state is parameterized by $\theta = \pi/4$, $\phi = \pi/4$.

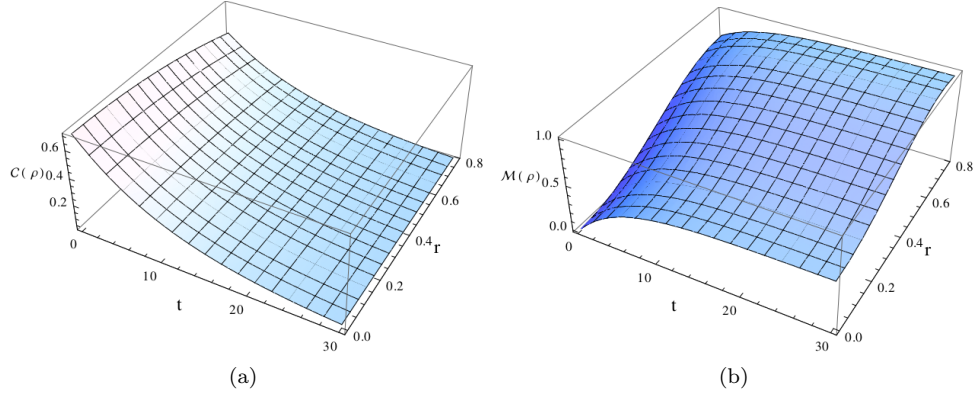


FIG. 15: Action of QND channel on (a) Coherence (b) Mixedness plotted against time (t) and Unruh parameter (r). The bath parameters are $a = 0$, $\omega_0 = 1$, $\gamma = 0.5$, $T = 0.5$, $s = 0.5$ and the input state is parameterized by $\theta = \pi/4$, $\phi = \pi/4$.

B. SGAD Channel

The analytical expressions for coherence and mixedness of the Unruh channel under the influence of the SGAD noise is

$$\mathcal{C}(\rho) = \cos r \sin \theta \sqrt{(p_1 \sqrt{1-\alpha} + p_2 \sqrt{(1-\mu)(1-\nu)})^2 + p_2^2 \mu \nu + 2 \cos(2\phi - \phi_s) \sqrt{\mu \nu} (p_1 \sqrt{1-\alpha} + p_2 \sqrt{(1-\mu)(1-\nu)})}, \quad (34)$$

$$\begin{aligned} \mathcal{M}(\rho) = & 2 \left(1 - \left(\cos \frac{\theta}{2} ((p_1 + p_2 - p_1 \alpha - p_2 \mu) \cos^2 r + p_2 \nu \sin^2 r) + p_2 \nu \sin^2 \frac{\theta}{2} \right)^2 \right. \\ & - \left((p_1 \alpha + p_2 \mu) \cos^2 r \cos^2 \frac{\theta}{2} + (p_1 + p_2 - p_2 \nu) (\cos^2 \frac{\theta}{2} \sin^2 r + \sin^2 \frac{\theta}{2}) \right)^2 \\ & - \frac{1}{2} e^{-i\phi - i(\phi + \phi_s)} \left(e^{i\phi_s} (p_1 \sqrt{1-\alpha} + p_2 \sqrt{1-\mu} \sqrt{1-\nu}) + e^{2i\phi} p_2 \sqrt{\mu \nu} \right) \times \\ & \left. \left(e^{2i\phi} (p_1 \sqrt{1-\alpha} + p_2 \sqrt{1-\mu} \sqrt{1-\nu}) + e^{i\phi_s} p_2 \sqrt{\mu \nu} \right) \cos^2 r \sin^2 \theta \right), \end{aligned} \quad (35)$$

respectively. From Fig. 16(a), it is observed that for a certain range of temperature T , coherence \mathcal{C} increases with squeezing s while in another range, it decreases with s , in consistence with the quadrature nature of squeezing.

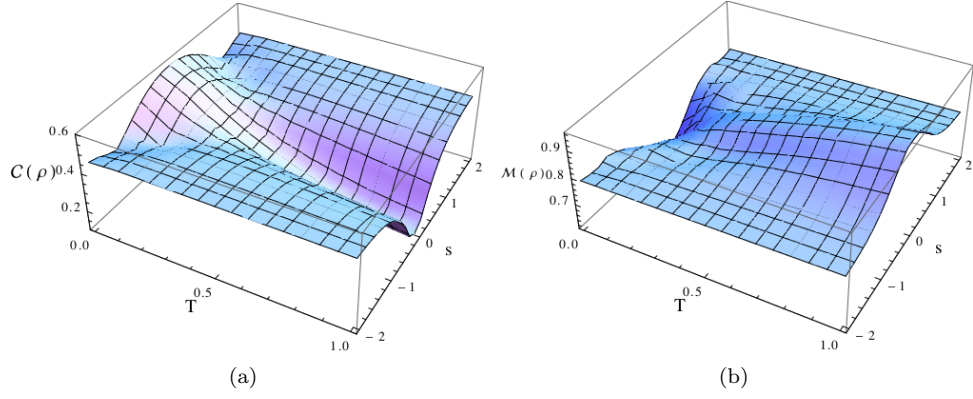


FIG. 16: Action of SGAD channel on (a) Coherence (b) Mixedness plotted against bath squeezing (s) and temperature(T). The bath parameters are $\phi_s = 0$, $\omega_0 = .1$, $\gamma = 0.1$, $t = 2$, $r = \pi/8$ and the input state is parameterized by $\theta = \pi/4$, $\phi = \pi/4$.

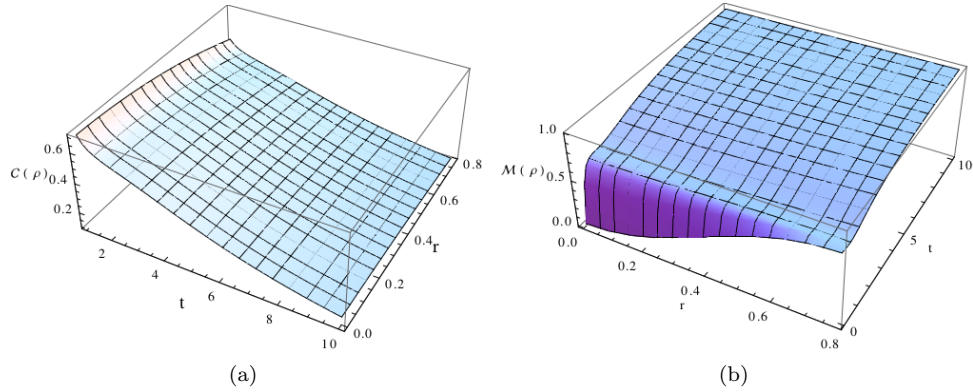


FIG. 17: (a) Variation of Coherence due to action of SGAD channel w.r.t time (t) and Unruh parameter (r). (b) Plot of Mixedness against time (t) and Unruh parameter (r). The bath parameters are $\phi_s = 0$, $\omega_0 = .1$, $\gamma = 0.1$, $T = 0.5$, $s = 0.5$ and the input state is parameterized by $\theta = \pi/4$, $\phi = \pi/4$.

Also, finite s brings a notion of stability in the behavior of coherence \mathcal{C} as a function of external temperature T . Thus, squeezing s once again emerges as a useful resource. The expected increase in mixing \mathcal{M} with increase in T is observed in Fig. 16(b). From Fig. 17, it can be seen that coherence decreases with increase in t and r whereas mixedness increases rapidly with t .

From Figs. 18 and 19, it is clear that the inequality Eq. (31) is respected for both QND and SGAD noises, respectively. In particular, from Fig. 18(a), due to the action of QND noise, it can be seen that for $t = 2$ and $r = \pi/8$, by varying parameters T and s we cannot get any MCMS as the inequality is not saturated. However, fixing T and s to 0.5 and varying r , MCMS can be achieved, as can be seen from Fig. 18(b). For the case of SGAD noise, Fig. 19(a) depicts that for $t = 2$ and $r = \pi/8$, by varying the parameters T and s MCMS states can be attained. Also, by fixing T and s to 0.5 and varying r and t , MCMS can be achieved as can be seen from Fig. 19(b).

VI. CONCLUSIONS

We show that the effect of Unruh acceleration on a qubit is similar to the action of an amplitude damping channel, where the damping parameter is determined by the acceleration, and thus by the Unruh temperature. Since the amplitude damping channel arises from interaction with a vacuum, this suggests that the Unruh temperature should be regarded as a factor that modifies the system's interaction strength rather than as the temperature of the damping environment. We study how environmentally induced decoherence modifies the effect of the Unruh channel, essentially by investigating the degradation of quantum information, as quantified by measures such as nonlocality, mixed-state

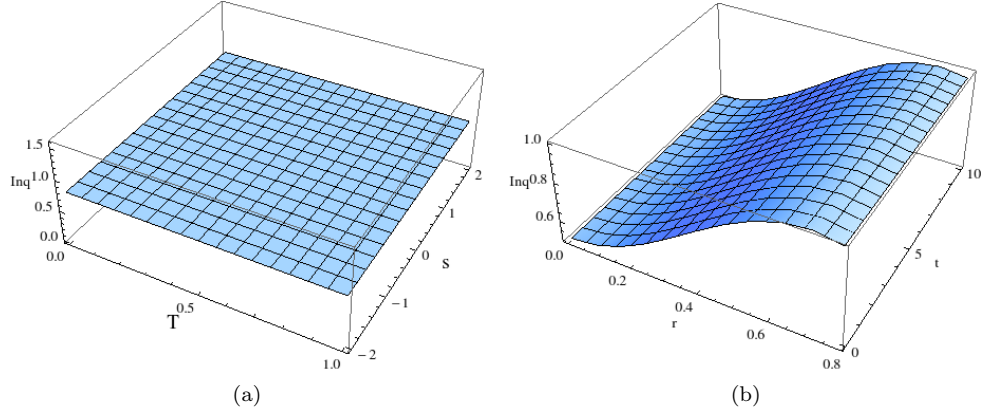


FIG. 18: Plots of inequality (Inq) in Eq. (31) due to action of QND (a) w.r.t parameters T and s with $t = 2$ and $r = \pi/8$, (b) against time (t) and Unruh parameter (r) with $T = 0.5$, $s = 0.5$. The bath parameters are $\phi_s = 0$, $\omega_0 = 0.1$, $\gamma = 0.1$ and the input state parameterized by $\theta = \pi/4$, $\phi = \pi/4$.

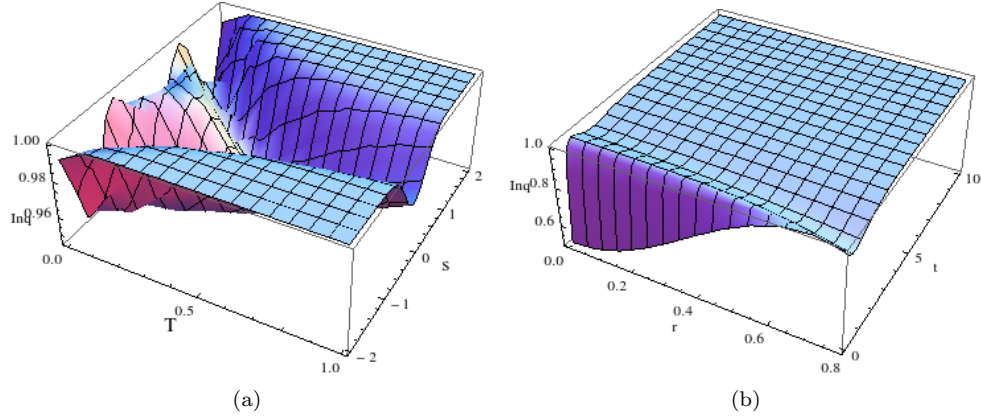


FIG. 19: Plot of inequality (Inq) in Eq. (31) due to action of SGAD channel (a) w.r.t parameters T and s with $t = 2$ and $r = \pi/8$, (b) against time (t) and Unruh parameter (r) with $T = 0.5$, $s = 0.5$. The bath parameters are $\phi_s = 0$, $\omega_0 = 0.1$, $\gamma = 0.1$ and the input state parameterized by $\theta = \pi/4$, $\phi = \pi/4$.

entanglement, teleportation fidelity, coherence and a discord-like quantity. The differing effects of an environment that interacts dissipatively or non-dissipatively are noted. In particular, the latter is shown to lead to a non-Pauli channel of rank 3. Further, useful parameters characterizing channel performance such as gate and channel fidelity are applied here to the Unruh channel, both with and without external influences. Squeezing is shown to be a useful resource in a number of scenarios. We hope this work is a contribution towards the development of relativistic quantum technologies.

-
- [1] M. Czachor, Phys. Rev. A **55**, 72 (1977).
 - [2] A. Peres, P. F. Scudo and D. R. Terno, Phys. Rev. Lett. **88**, 230402 (2002).
 - [3] P. Caban, J. Rembielinski and M. Włodarczyk, Ann. of Phys. **330**, 263 (2013).
 - [4] S. Banerjee, A. K. Alok and R. MacKenzie, arXiv:1409.1034 [hep-ph].
 - [5] A. K. Alok, S. Banerjee and S. U. Sankar, arXiv:1411.5536 [quant-ph].
 - [6] S. Banerjee, A. K. Alok, R. Srikanth and B. C. Hiesmayr, Eur. Phys. J. C **75**, 487 (2015).
 - [7] I. Fuentes, R. B. Mann, E. M-Martinez and S. Moradi, Phys. Rev. D **82**, (2010).
 - [8] P. C. W. Davies, J. Phys. A **8** 609 (1975); W. G. Unruh, Phys. Rev. D **14** 870 (1976).
 - [9] L. C. B. Crispino, A. Higuchi and G. E. A. Matsas, Rev. Mod. Phys. **80** 787 (2008).

- [10] P. M. Alsing and G. J. Milburn, Phys. Rev. Lett. **91**, 180404 (2003).
- [11] P. M. Alsing, I. Fuentes-Schuller, R. B. Mann and T. E. Tessier, Phys. Rev. A **74**, 032326 (2006).
- [12] Z. Tian, J. Wang and J. Jing, Annals Phys. **332**, 98 (2013).
- [13] A. R. Lee and I. Fuentes, Phys. Rev. D **89**, 085041 (2014).
- [14] A. Peres and D. R. Terno, Rev. Mod. Phys. **76**, 93 (2004).
- [15] P. D. Nation, J. R. Johansson, M. P. Blencowe and F. Nori, Rev. Mod. Phys. **84**, 1 (2012).
- [16] N. Friis, A. R. Lee, K. Truong, C. Sabin, E. Solano, G. Johansson and I. Fuentes, Phys. Rev. Lett. **110**, 113602 (2013).
- [17] C. K. Andersen and K. Mølmer, Phys. Rev. A **91**, 023828 (2015).
- [18] D. E. Bruschi, A. Dragan, A. R. Lee, I. Fuentes and J. Louko, Phys. Rev. Lett. **111**, 090504 (2013).
- [19] S. Felicetti et al., Phys. Rev. Lett. **113**, 093602 (2014).
- [20] I. M. de Sousa and A. V. Dodonov, J. Phys. A **48**, 245302 (2015).
- [21] S. Felicetti et al., Phys. Rev. B **92**, 064501 (2015).
- [22] D. E. Bruschi et al., Scientific Reports DOI: 10.1038/srep18349.
- [23] J. Lindkvist et al., Phys. Rev. A **90**, 052113 (2014).
- [24] E. M-Martnez, I. Fuentes and R. B. Mann, Phys. Rev. Lett. **1067**, 131301 (2011).
- [25] M. Aspachs, G. Adesso and I. Fuentes, Phys. Rev. Lett. **105**, (2010).
- [26] Y. Yao et. al., Phys. Rev. A **89**, 042336 (2014).
- [27] S. Banerjee, A. K. Alok and S. Omkar, arXiv:1511.03029 [quant-ph].
- [28] S. Banerjee and R. Ghosh, J. of Phys. A: Math. and Theor. **40**, 13735 (2007); S. Banerjee, J. Ghosh and R. Ghosh, Phys. Rev. A **75**, 062106 (2007); S. Banerjee and R. Srikanth, Eur. Phys. J. D **46**, 335 (2008).
- [29] V. B. Braginsky and Yu. I. Vorontsov, Usp. Fiz. Nauk **114**, 41 (1974) [Sov. Phys. Usp. **17**, 644 (1975)].
- [30] C. M. Caves, K. S. Thorne, R. W. P. Drever, V. D. Sandberg, and M. Zimmerman, Rev. Mod. Phys. **52**, 341 (1980).
- [31] R. Srikanth and S. Banerjee, Phys. Rev. A **77**, 012318 (2008).
- [32] S. Omkar, R. Srikanth and S. Banerjee, Quantum Information Processing **12**, 3725 (2013).
- [33] S. Omkar, S. Banerjee, R. Srikanth and A. K. Alok, arXiv:1408.1477 [quant-ph].
- [34] E. Maheshan, Quantum Inf. Comput. **11**, 0466 (2011).
- [35] M. D. Bowdrey, D. K. L. Oi, A. J. Short, K. Banaszek and J. A. Jones, Phys. Lett. A, **294**, 258 (2002).
- [36] M. A. Nielsen, Phys. Lett. A, **303**, 249 (2002).
- [37] N. Srinatha, S. Omkar, R. Srikanth, S. Banerjee, and A. Pathak, Quantum Inf. Comput. **13**, 59 (2012).
- [38] T. Baumgratz, M. Cramer, and M. B. Plenio, Phys. Rev. Lett. **113**, 140401 (2014).
- [39] A. Streltsov, U. Singh, H. S. Dhar, M. N. Bera and G. Adesso, Phys. Rev. Lett. **115**, 020403 (2015).
- [40] U. Singh, M. N. Bera, H. S. Dhar, and A. K. Pati, Phys. Rev. A **91**, 052115 (2015).
- [41] S. Khan and M. K. Khan, J. of Phys. A: Math. and Theor. **44**, 045305 (2011).
- [42] Y. Yao et. al., Phys. Rev. A **89**, 042336 (2014).
- [43] M. D. Choi, *Linear Algebra and Its Applications* **10**, 285 (1975).
- [44] D. W. Leung, J. Math. Phys. **44**, 528 (2003); T. F. Havel, J. Math. Phys. **44**, 534 (2003).
- [45] J. F. Clauser, and A. Shimony, Rep. Progr. Phys. **41**, 1881 (1978).
- [46] J. F. Clauser, M. A. Horne, A. Shimony, and R. A. Holt, Phys. Rev. Lett. **23**, 880 (1969).
- [47] A. Aspect, J. Dalibard, and G. Roger, Phys. Rev. Lett. **49**, 1804 (1982).
- [48] A. Peres, Phys. Rev. Lett. **77**, 1413 (1996).
- [49] R. Horodecki, M. Horodecki, and P. Horodecki, Phys. Lett. A **222**, 21 (1996).
- [50] M. Horodecki, P. Horodecki, and R. Horodecki, Phys. Lett. A **223**, 1 (1996).
- [51] W. K. Wootters, Phys. Rev. Lett. **80**, 2245 (1998).
- [52] C. H. Bennett, G. Brassard, C. Crepeau, R. Jozsa, A. Peres, and W. K. Wootters, Phys. Rev. Lett. **70**, 1895 (1993).
- [53] S. Popescu, Phys. Rev. Lett. **72**, 797 (1994).
- [54] H. Ollivier, and W. H. Zurek, Phys. Rev. Lett. **88**, 017901 (2001); L. Henderson, and V. Vedral, J. Phys. A **34**, 6899 (2001).
- [55] S. Luo, Phys. Rev. A **77**, 042303 (2008).
- [56] N. A. Peters, T.-C. Wei and P. G. Kwiat, Phys. Rev. A **70**, 052309 (2004).
- [57] E. Maheshan, Quantum Inf. Comput. **11**, 0466 (2011).
- [58] M. D. Bowdrey, D. K. L. Oi, A. J. Short, K. Banaszek and J. A. Jones, Phys. Lett. A **294**, 258 (2002).
- [59] M. A. Nielsen, Phys. Lett. A **303**, 249 (2002).